

F. Gao  
Y. Wang  
Y. Qiu  
Y. Li  
Y. Sha  
L. Lai  
H. Wu

# $\beta$ -turn formation by a six-residue linear peptide in solution

## Authors' affiliations:

F. Gao, Y. Li, Y. Sha\* and L. Lai, Institute of Physical Chemistry, Peking University, Beijing, China; and \*Department of Biophysics, School of Basic Medical Sciences, Peking University, Beijing, China.

Y. Wang and H. Wu, State Key Laboratory of Bioorganic and Natural Products Chemistry, Shanghai Institute of Organic Chemistry, Chinese Academy of Sciences, Shanghai, China.

Y. Qiu, Department of Biophysics, School of Basic Medical Sciences, Peking University, Beijing, China.

## Correspondence to:

Dr Yinlin Sha  
Biochemistry Building 204  
Department of Biophysics  
Peking University Health Science Center  
Beijing 100083  
China  
Tel.: 86-10-823-32096  
Fax: 86-10-823-32096  
E-mail: shyl@bjmu.edu.cn

## Dates:

Received 6 November 2001  
Revised 24 January 2002  
Accepted 15 March 2002

## To cite this article:

Gao, F., Wang, Y., Qiu, Y., Li, Y., Sha, Y., Lai, L. & Wu, H.  $\beta$ -turn formation by a six-residue linear peptide in solution.

*J. Peptide Res.*, 2002, **60**, 75–80.

Copyright Blackwell Munksgaard, 2002

ISSN 1397-002X

**Key words:**  $\beta$ -turn; CD; FT-IR; NMR

**Abstract:** A model peptide AAGDYY-NH<sub>2</sub> (B1), which is found to adopt a  $\beta$ -turn conformation in the TEM-1  $\beta$ -lactamase inhibitor protein (BLIP) in the TEM-1/BLIP co-crystal, was synthesized to elucidate the mechanism of its  $\beta$ -turn formation and stability. Its structural preferences in solution were comprehensively characterized using CD, FT-IR and <sup>1</sup>H NMR spectroscopy, respectively. The set of observed diagnostic NOEs, the restrained molecular dynamics simulation, CD and FT-IR spectroscopy confirmed the formation of a  $\beta$ -turn in solution by the model peptide. The dihedral angles [( $\phi_3$ ,  $\phi_3$ ) ( $\phi_4$ ,  $\phi_4$ )] of [(-52°, -32°) (-38°, -44°)] of Gly-Asp fragment in the model peptide are consistent with those of a type III  $\beta$ -turn. In a conclusion, the conformational preference of the linear hexapeptide B1 in solution was determined, and it would provide a simple template to study the mechanism of  $\beta$ -turn formation and stability.

Understanding the mechanism of secondary structure formation and stability is an essential part of solving the protein-folding puzzle (1–3). In the past, the structures of protein fragments and designed peptides have been widely explored by spectroscopic analysis, including nuclear magnetic resonance, infrared spectra and circular dichroism measurements, to obtain information on secondary structure formation and stability (4–6). Occurring as a regular secondary structural element,  $\beta$ -turns are prevalent in globular proteins, and may also be possible sites for nucleation in protein folding. Although much is known about the characteristics of  $\beta$ -turns in proteins (7,8), many questions remain unanswered about what factors determine  $\beta$ -turn formation and stability, and what role they play in protein folding. Recently, several peptide models that

adopt  $\beta$ -hairpin conformations have been developed to investigate  $\beta$ -sheet formation and stability (9–11). However, it may be problematic to identify the interactions that stabilize  $\beta$ -turns with  $\beta$ -hairpin peptide models, because the interstrand interactions observed in a  $\beta$ -hairpin may enhance  $\beta$ -turn formation and stability.

Here, we show that a functional hairpin loop AAGDYY-NH<sub>2</sub> (B1) from TEM-1  $\beta$ -lactamase inhibitor protein (12–14) co-crystallized with TEM-1  $\beta$ -lactamase exists in solution with a  $\beta$ -turn conformation in the absence of the protein context. Our experimental results show that the short linear hexapeptide B1 can form a  $\beta$ -turn conformation in solution, and the conformational potency of peptide backbones and environment would be the determinants for its formation and also support the concept that  $\beta$ -turns can be stabilized mainly by local interactions rather than medium- or long-range hydrophobic or electrostatic interactions. Moreover, the relatively rigid backbone of the model peptide is expected to be a useful template for the *de novo* design of peptide inhibitors of TEM-1  $\beta$ -lactamase.

## Materials and Methods

### Peptide synthesis and purification

Peptide B1 (AAGDYY-NH<sub>2</sub>) was synthesized on a 0.2-mmol scale by solid-phase peptide synthesis strategy using Fmoc chemistry (15). Cleavage of the peptide from Rink resin and removal of all side chain-protecting groups were achieved in trifluoroacetic acid solution. The crude peptide was purified by reversed-phase high-performance liquid chromatography (RP-HPLC, Gilson) on a ZORBAX C<sub>18</sub> column with gradients of water/acetonitrile containing 0.1% trifluoroacetic acid. Peptide homogeneity and identity were analyzed by analytical HPLC, and matrix-assisted laser desorption time-of-flight mass spectroscopy (MALDITOF MS), respectively.

### Far-UV circular dichroism spectroscopy

The CD spectrum was recorded on a Jobin-Yvon CD6 spectrometer and was the average of three scans corrected by subtracting a spectrum of the appropriate solution in the absence of peptide recorded under identical conditions. Each scan in the range 190–250 nm was obtained by taking data points every 0.5 nm, with integration time 0.5 s and

a 2-nm band width. A cell with a path length of 0.1 mm was used.

### Infrared spectroscopy

Residual trifluoroacetic acid was removed from the samples after peptide synthesis and HPLC purification by at least three lyophilization–solubilization cycles in 10 mM HCl solution. The peptide B1 was analyzed in D<sub>2</sub>O by IR at 5 mg/mL, at pH 7.0 and 20°C, using a Bio-Rad FTS165 spectrometer equipped with a DTGS detector and a cell pathlength 25  $\mu$ m. Typically, 400 scans were averaged after subtraction of the buffer contribution. After Fourier transforming with a triangular apodization function, curve fitting was performed with the Bio-Rad WIN-IR CURVEFIT.AB program.

### NMR spectroscopy and dynamic simulation

All NMR experiments were recorded at 24°C on a Varian Unity Inova 600 spectrometer. The sample concentration was 3.5 mM in DMSO-*d*<sub>6</sub> solvent. Two-dimensional total correlation spectroscopy (TOCSY) (16), and nuclear Overhauser enhancement spectroscopy (NOESY) (17) were recorded using the time-proportional phase incrementation of the first pulse (18). The TOCSY spectrum was acquired using the MELV-17 pulse sequence with a 80-ms mixing time (19) and the NOESY spectrum (Fig. 3) was recorded with a 600-ms mixing time and displayed in the phase-sensitive mode. Usually, 256×2048 data points were collected and for each block, 64 transients were collected for two-dimensional experiments. The experimental data were acquired and processed using the VNMR 6.1B program on a SUN sparc station ultra 170 computer. The processed data were analyzed using XEASY (20) for visualization of NMR data, peak-picking and peak-integration using a Silicon Graphics Indigo R 5000 computer.

Assignment of resonances of peptide B1 was accomplished by two steps (spin system identification and sequential assignment) according to the general procedure described by Wüthrich (21). The value of cross-peaks in the NOESY spectrum was used to generate the distance constraints. The preliminary structures were created using DYANA (22) on a silicon graphic Indy R 5000 computer. The 17 structures with lowest target function, that resulted from calculations with the final input data set starting with 100 random structures using torsion-space molecular dynamics annealing, were subjected to restrained energy minimization (REM) performed with the SANDER module of the AMBER

5.0 package (23,24), using the AMBER all-atom parametrization. Of the 17 structures obtained, 13 that were most consistent with the NMR data were selected.

## Results and Discussion

We synthesized a six-residue linear peptide with potential to form  $\beta$ -turn structure in solution and investigated its structural preferences by CD, FT-IR and  $^1\text{H}$  NMR spectroscopy, respectively.

The far-UV CD spectrum of  $\beta$ -turn has been identified as a weak red-shifted positive  $n \rightarrow \pi^*$  band near 225 nm, a strong positive  $\pi \rightarrow \pi^*$  transition between 200 and 205 nm, and a strong negative band between 180 and 190 nm (25). Figure 1 shows the CD spectrum of peptide B1 in 50 mM phosphate buffer at 20°C. The general characteristics of the CD spectrum with a negative band at 193 nm and two positive bands near 204 and 228 nm are consistent with those of reported  $\beta$ -turn CD as described previously (25), indicating  $\beta$ -turn formation by peptide B1 in aqueous solution. However, overlapping far-UV CD signal from the aromatic side chains may exist in Fig. 1, because free Tyr in solution can also have a far-UV CD signal similar to  $\beta$ -turn structure (26). It is necessary to identify the origins of the obtained far-UV CD characteristics of peptide B1 in aqueous solution, and subsequently, far-UV CD spectra of B1 and its derivative sequences composing Tyr-Tyr fragment were compared (data not shown). At least two of the derivative sequences exhibited different CD characteristics with that of B1 indicate that it would be  $\beta$ -turn structure but not Tyr aromatic side chain contributes greatly to the CD characteristics.

The aromatic CD spectrum (near-UV CD) may be used to examine the occurrence of secondary and tertiary

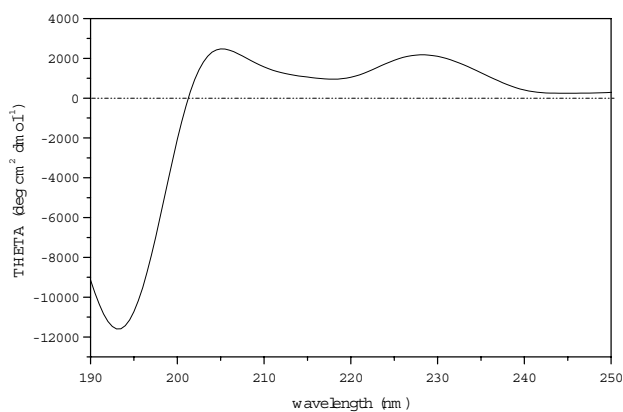


Figure 1. The far-UV CD spectrum of peptide B1 (1 mg/mL) in 50 mM phosphate buffer at 20°C.

structure in peptides and proteins (27). Weak, monotonous spectrum suggests usually a disordered and fluctuating structures. The near-UV CD spectra of peptide B1 suggested the presence of unique side-chain packing and asymmetric environments about the aromatic amino acid Tyr at lower temperature in aqueous solution and at higher temperature in DMSO/water mixed solvent (Fig. 2). The near-UV CD spectra as a function of temperature (data not shown) also indicated that the Tyr aromatic side chain gradually adopted a variety of different orientations when temperature increased, as observed by an averaging of CD signals having weaker intensity. The CD experiments supported the theory that peptide B1 existed in aqueous solution as a  $\beta$ -turn structure exhibiting CD characteristics distinctly different from the spectra of Tyr aromatic side chains.

The aqueous solution structure of peptide B1 was also investigated using infrared spectroscopy by examining the conformation-sensitive bands arising from the peptide bond. Figure 3 shows the curve-fitted amide I band region

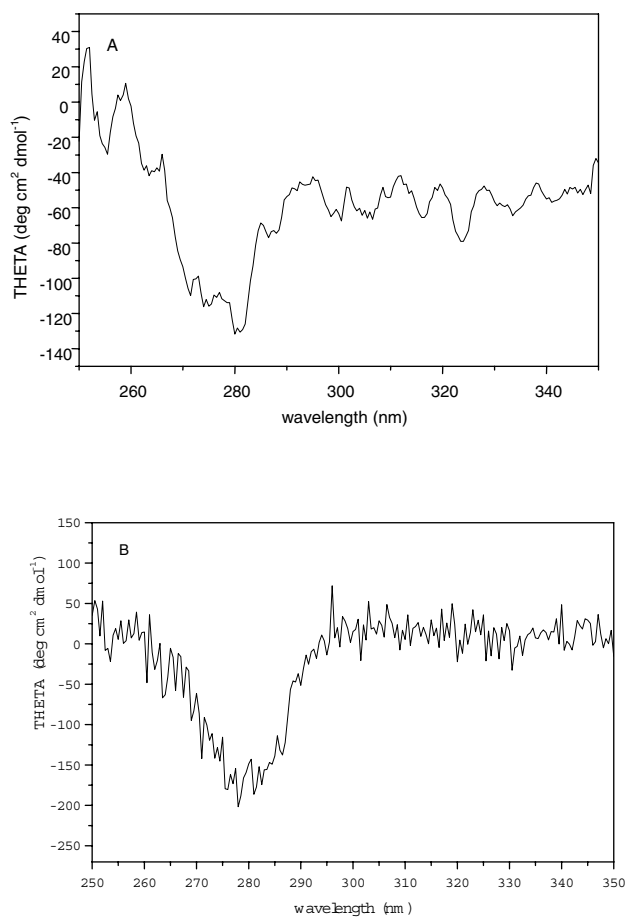


Figure 2. [A] The near-UV CD spectrum of peptide B1 in phosphate-buffered saline at 10°C. [B] The near-UV CD spectrum of peptide B1 in DMSO/H<sub>2</sub>O (1 : 1 v/v) solution at 24°C.

of peptide B1 in 50 mM phosphate ( $D_2O$ ) buffer. Band position, assignment and percentages (28) of the spectral components are shown in Table 1. The two bands, located at 1668 and 1681  $cm^{-1}$ , are indicative of the presence of  $\beta$ -turn structure, and the absorptions at 1613  $cm^{-1}$  may arise from side-chain vibrations of tyrosine. The band at 1648  $cm^{-1}$  can be assigned as overlapping absorptions of  $\beta$ -turn and unordered conformations. Considering the CD and NMR results, it is reasonable to conclude that the main contribution of band 1648  $cm^{-1}$  is from  $\beta$ -turn conformation. Although the quantitative values (Table 1) are based on various assumptions inherent in curve-fitting routines, they provide good estimates, particularly when used in a comparative manner (29).

NMR experiments were initially carried out in water for comparison with the CD and IR data and for a more detailed characterization of the conformational preferences and stability of peptide B1. However, many negative NOEs were observed in the NOESY spectrum, indicative of effective correlation times that were large compared with  $1/\omega$ , i.e.  $\tau \gg 0.3$  ns in water (30). Subsequently, NMR experiments were performed in  $DMSO-d_6$ . Although several NMR parameters may be used, it is generally recognized that the pattern of diagnostic NOEs, in particular long- and medium-range NOEs, are the most conclusive evidence of secondary structure. The complete  $^1H$  NMR assignments of B1 are given in Table 2, and Fig. 4

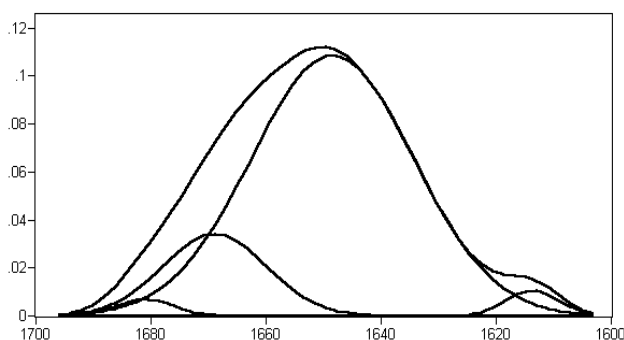


Figure 3. Decomposition of the amide I band of peptide B1 in 50 mM phosphate buffer ( $D_2O$ ) at 20°C.

Table 1. Band position, percentage area and assignment of FT-IR spectrum for peptide B1

Band position ( $cm^{-1}$ )	% area	Assignment
1681	2	$\beta$ -turn
1668	16	$\beta$ -turn
1648	79	$\beta$ -turn+unordered
1613	3	Tyr residues

shows the observed representative cross-peaks in the NOESY experiment, including  $\alpha N(i, i+2)$  NOE cross-peak between residues Gly<sup>3</sup>-Tyr<sup>5</sup>,  $\alpha N(i, i+1)$  and between residues Asp<sup>4</sup>-Tyr<sup>5</sup> and Gly<sup>3</sup>-Asp<sup>4</sup>, as well as intense  $NN(i, i+1)$  NOE cross-peaks between residues Asp<sup>4</sup>-Tyr<sup>5</sup> and Gly<sup>3</sup>-Asp<sup>4</sup> (very close to diagonal peak, Fig. 5).

Although NOEs cannot be rigorously interpreted in terms of a unique structure due to conformational averaging (31), it is not uncommon (32) to look for a model structure compatible with the experimental NOEs using distance geometry and energy minimization. The best 12 calculated structures of peptide B1 shown in Fig. 6 qualitatively account for the observed patterns of NOEs, and are consistent with the  $\alpha N(i, i+2)$  and  $NN(i, i+1)$  NOEs involving residues 2–5. The RMSD of the backbone heavy atoms of the structures is 0.28 Å. This value is relatively small considering the potential for conformational averaging in a small peptide and the limited possibilities for obtaining NOE restraints in peptide B1 (33). The superimposition of the structures over the backbone indicates

Table 2. NMR assignments for peptide B1 in DMSO solution at 24°C ( $\delta$ , p.p.m)

Residues	NH	$\alpha$ H	$\beta$ H	$\delta$ H	$\epsilon$ H
Ala <sup>1</sup>		3.85	1.32		
Ala <sup>2</sup>	8.57	4.39	1.26		
Gly <sup>3</sup>	8.18	3.76, 3.68			
Asp <sup>4</sup>	8.19	4.56	2.66, 2.42		
Tyr <sup>5</sup>	7.90	4.27	2.80, 2.64	6.93, 6.93	6.61, 6.61
Tyr <sup>6</sup>	7.84	4.29	2.87, 2.71	7.01, 7.01	6.65, 6.65

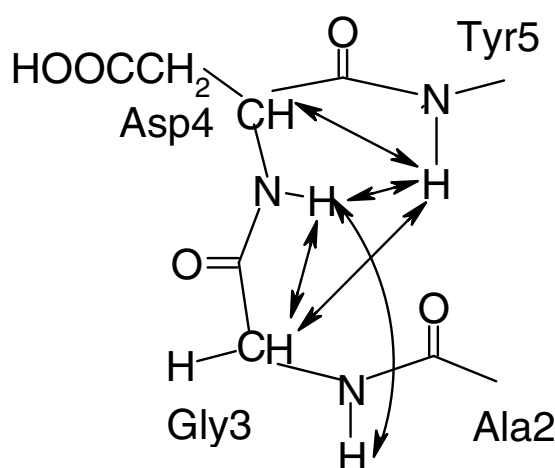


Figure 4. Region of 600-MHz NOESY spectrum of peptide B1 at 24°C in DMSO solution [A: Gly<sup>3</sup> C $\alpha$ H $\leftrightarrow$ Tyr<sup>5</sup> NH, B: Asp<sup>4</sup> NH $\leftrightarrow$ Tyr<sup>5</sup> NH, C: Gly<sup>3</sup> NH $\leftrightarrow$ Asp<sup>4</sup> NH, D: Gly<sup>3</sup> C $\alpha$ H $\leftrightarrow$ Asp<sup>4</sup> NH, E: Asp<sup>4</sup> C $\alpha$ H $\leftrightarrow$ Tyr<sup>5</sup> NH].

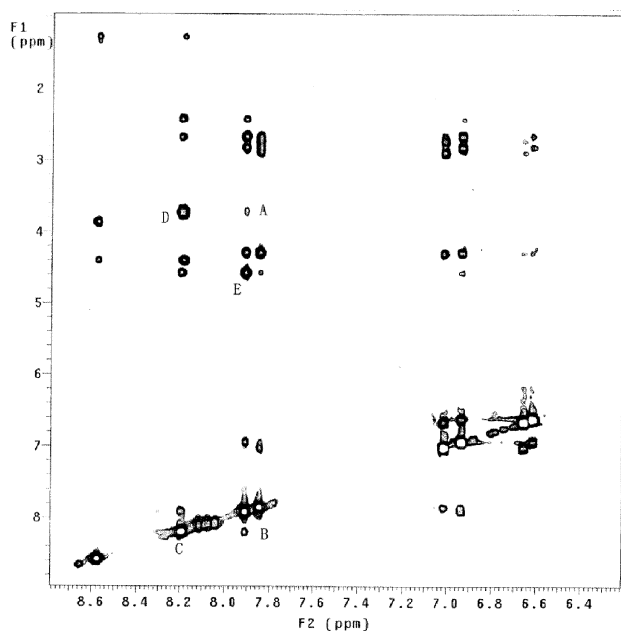


Figure 5. The key NOEs observed for peptide B1.



Figure 6. The 12 best superimposed structures of B1 compatible with the patterns of NOEs observed.

that peptide B1 forms a  $\beta$ -turn with dihedral angles  $[(\phi_3, \psi_3)$   $(\phi_3, \psi_3)]$  of  $[(-52^\circ, -32^\circ)$   $(-38^\circ, -44^\circ)]$ , corresponding to a typical type III  $\beta$ -turn (34). The final calculated structures exhibit a hydrogen bond (35) between the Ala<sup>2</sup> carbonyl oxygen and the Tyr<sup>5</sup> amide hydrogen that is characteristic of  $\beta$ -turn formation. However, evidence for the existence of the hydrogen bond was not observed in the H/D interchange experiment, which can be explained by the presence of a fast conformational equilibrium between  $\beta$ -turn and unordered conformations (28) in the short peptide system.

The model peptide B1 exists in DMSO solution with type III turn conformation; however, the same peptide sequence adopts a type II' turn in the TEM-1/BLIP co-crystal. The observed conformational change of peptide B1 means that environment is an important determinant for  $\beta$ -turn formation.

What are the origins of  $\beta$ -turn formation and stability in solution? The model peptide B1, owing to its simplicity, is a good candidate for dissecting and quantifying the different interactions contributing to  $\beta$ -turn formation and stability. It has been suggested that the conformation of a given peptide sequence is governed by a complex balance between intrinsic  $\phi$ ,  $\psi$  propensities of the various amino acids and their abilities to form local hydrophobic and electrostatic side chain to side chain or side chain to backbone interactions (36). However, in our case, the NMR studies indicate that there does not exist any interstrand structure-stabilizing interactions between the side chains of Ala<sup>1</sup> and Tyr<sup>6</sup>, or Ala<sup>2</sup> and Tyr<sup>5</sup>, as no long-range NOEs were observed indicating that these residues were in close proximity to each other. These observations would suggest that the conformational propensity of the peptide backbone could contribute greatly to  $\beta$ -turn formation. It can be expected that the entropy loss in fixing residues is less obvious in the process of forming a conformation by a small peptide with relatively rigid peptide backbone. Therefore, it seems that for peptide B1, turn residues Ala-Gly-Asp-Tyr are responsible for stabilizing the structure. The  $\beta$ -turn-forming tendency of the Gly-Asp fragment, instead of hydrophobic or electrostatic interactions, provides the stabilization energy required for a conformation to be formed. The results of our studies also show that environment, sequence context and solution properties are important determinants for  $\beta$ -turn formation, and in particular the type of  $\beta$ -turn.

The fact that peptide B1 adopts  $\beta$ -turn conformation in solution implicates that some small peptides can exist in solution with a conformational preference instead of an unordered states. Further studies of the small structure-formed peptide fragments may provide insight into the origins of  $\beta$ -turn formation and stability toward a better understanding of protein folding mechanisms.

**Acknowledgments:** We gratefully acknowledge professor Peter Guntert for the use of the DYANA 1.5 program and Peter Kollman for the use of the AMBER 5.0 package. This work was supported by Ministry of Science and Technology (970211006) and NSFC (20103001).

## References

1. Blanco, F.J., Ramirez-Alvarado, M. & Serrano, L. (1998) *Curr. Opin. Struct. Biol.* **8**, 107–111.
2. Pelton, J.T. & Mclean, L.R. (2000) *Anal Biochem.* **277**, 167–176.
3. Zerella, R., Chen, P.Y., Evans, P.A., Raine, A. & Williams, D.H. (2000) *Protein Sci.* **9**, 2142–2150.
4. Wishart, D.S., Sykes, B.D. & Richards, F.M. (1991) *J. Mol. Biol.* **222**, 311–333.
5. Heimburg, H., Esmann, M. & Marsh, D. (1997) *J. Biol. Chem.* **272**, 25685–25692.
6. Cabiaux, V., Brasseur, R., Wattiez, R., Falmagne, P., Ruyschaert, J.M. & Goormaghtigh, E. (1989) *J. Biol. Chem.* **264**, 4928–4938.
7. Haque, T.S., Little, J.C. & Gellman, S.H. (1994) *J. Am. Chem. Soc.* **116**, 4105–4106.
8. Srinivasa, R.R., Satish, K.A. & Padmanabhan, B. (1998) *J. Chem. Soc., Perkin Trans.* **2**, 137–143.
9. Blanco, F.J., Jimenez, M.A., Rico, M., Santoro, J., Herranz, J. & Nieto, J.L. (1993) *J. Am. Chem. Soc.* **115**, 5887–5888.
10. Searle, M.S., Williams, D.H. & Packman, L.C. (1995) *Nature Struct. Biol.* **2**, 999–1006.
11. Ramirez-Alvarado, M., Blanco, F.J. & Serrano, L. (1996) *Nature Struct. Biol.* **3**, 604–612.
12. Strynadka, N.C., Jensen, S.E., Johns, K., Blanchard, H., Page, M., Matagne, A., Frere, J.M. & James, M.N. (1994) *Nature* **368**, 657–660.
13. Strynadka, N.C., Adachi, H., Jensen, S.E., Johns, K., Sielecki, A., Betzel, C., Sutoh, K. & James, M.N. (1992) *Nature* **359**, 700–705.
14. Strynadka, N.C., Jensen, S.E., Alzari, P.M. & James, M.N. (1996) *Nature Struct. Biol.* **3**, 290–297.
15. Fields, G.B. & Noble, R.L. (1990) *Int. J. Peptide Protein Res.* **35**, 161–214.
16. Griesinger, C., Otting, G., Wuthrich, K. & Ernst, R.R. (1988) *J. Am. Chem. Soc.* **110**, 7870–7872.
17. Jeener, J., Meier, B.H., Bachmann, P. & Ernst, R.R. (1979) *J. Chem. Phys.* **71**, 4546–4553.
18. Drobny, G., Pines, A., Sinton, S., Weitekamp, D. & Wemmer, D. (1979) *Faraday Symp. Chem. Soc.* **13**, 49–55.
19. Bax, A. & Davis, D.G. (1985) *J. Magn. Reson.* **65**, 355–366.
20. Bartels, C., Xia, T., Billeter, M., Guntert, P. & Wuthrich, K. (1995) *J. Biomol. NMR* **6**, 1–10.
21. Wuthrich, K. (1986) *NMR of Proteins and Nucleic Acids*. Wiley, New York.
22. Guntert, P., Mumenthaler, M. & Wuthrich, K. (1997) *J. Mol. Biol.* **273**, 283–298.
23. Weiner, S.J. & Kollman, P.A. (1981) *J. Comput. Chem.* **2**, 287–309.
24. Weiner, S.J., Kollman, P.A., Nguyen, D.T. & Case, D.A. (1986) *J. Comput. Chem.* **7**, 230–252.
25. Rodger, A. & Norden, B. (1997) *Circular Dichroism and Linear Dichroism*. Oxford University Press, Oxford.
26. Lu, Z.-X., Cui, T. & Shi, Q.-L. (1987) *CD and ORD Application in Molecular Biology*. China Science Press, Beijing.
27. Blondelle, S.E., Esteve, V., Celda, B., Pastor, M.T. & Perez-paya, E. (2000) *J. Peptide Res.* **56**, 121–131.
28. Arrondo, J.L., Blanco, F.J., Serrano, L. & Goni, F.M. (1996) *FEBS Lett.* **384**, 35–37.
29. Guijarro, J.I., Jackson, M., Chaffotte, A.F., Delepierre, M., Mantsch, H.H. & Goldberg, M.E. (1995) *Biochemistry* **34**, 2998–3008.
30. Andrew, N.L., Lane, A.N., Hays, L.M., Feeney, R.E., Crowe, L.M. & Crowe, J.H. (1998) *Protein Sci.* **7**, 1555–1563.
31. Saulitis, J. & Liepins, E. (1990) *J. Magn. Reson.* **87**, 80–91.
32. Kemmink, J., Van Mierlo, C.P.M., Sheek, R.M. & Creighton, T.E. (1993) *J. Mol. Biol.* **230**, 312–322.
33. Sieber, V. & Moe, G.R. (1996) *Biochemistry* **35**, 181–188.
34. Lai, L.-H. (1993) *Protein Structure Prediction and Molecular Design*. Peking University Press, Beijing.
35. Stryer, L. (1988) *Biochemistry*, 3rd edn. W.H. Freeman, New York.
36. Guerois, P., Cordier-Ochsenbein, F., Baleux, F., Huynh-Dinh, T., Neumann, J.-M. & Sanson, A. (1998) *Protein Sci.* **7**, 1506–1515.